View Online
Dynamic Article Links

Energy & Environmental Science

Cite this: *Energy Environ. Sci.*, 2011, **4**, 935

www.rsc.org/ees

PAPER

Spherical core-shell $Li[(Li_{0.05}Mn_{0.95})_{0.8}(Ni_{0.25}Mn_{0.75})_{0.2}]_2O_4$ spinels as high performance cathodes for lithium batteries

Seung-Taek Myung,[a] Ki-Soo Lee,[bc] Dong-Won Kim,[c] Bruno Scrosati*[bd] and Yang-Kook Sun*[bc]

Received 22nd July 2010, Accepted 17th November 2010
DOI: 10.1039/c0ee00298d

Spinel-type, lithium manganese oxides, *e.g.* $LiMn_2O_4$, are very appealing electrodes for upgrading lithium batteries in terms of cost and environmental compatibility. Unfortunately, the practical use of these oxides has so far been hindered by some drawbacks, the most serious being the short life associated with the severe capacity fading on cycling, especially experienced at temperatures above ambient. In this work we report a new strategy for tackling this issue. The results reported here demonstrate that our approach, based on innovative core-shell electrode morphology, is very effective in improving the behaviour of lithium manganese spinel electrodes in lithium cells, by ensuring exceptional capacity stability upon cycling in temperature ranges where all the previous manganese based electrode materials inevitably failed. We show that our core-shell electrodes deliver a specific capacity of the order of 85 mAh g^{-1} in range of 3–4.3 V *vs.* Li/Li^+ with a retention of 97% over 100 cycles at 60 °C . To our knowledge, such high performance levels have not been met so far.

1. Introduction

The present concern on global warming urgently requires a large increase in the energy share provided by green, renewable energy sources, as well as a massive commercialization of sustainable vehicles. Both these actions rely on the availability of reliable energy storage systems, and highly efficient lithium batteries can in principle serve the purpose. However, in their present version these batteries are unable to meet the requirements of green energy plants or of hybrid or electric vehicles and thus, the renewal of the present chemistry by the development of advanced, low-cost, high-performance electrode materials, is mandatory.[1]

In this respect, very appealing candidates are spinel-type, lithium manganese oxides, *e.g.*, $LiMn_2O_4$. In fact, in view of their properties, that include material availability and environmental compatibility, these oxides appear as ideal cathode substitutes for the common, high-cost and partially toxic lithium cobalt oxide, $LiCoO_2$. Unfortunately, the wide practical use of the lithium manganese spinel electrode has so far been hindered by their severe capacity fading on cycling, especially when operating at temperatures above ambient, *e.g.*, above 40 °C.[2] This limiting phenomenon is due to the manganese dissolution, in turn associated with the disproportionate reaction of Mn^{3+}, *i.e.*: $2Mn^{3+} \rightarrow Mn^{2+} + Mn^{4+}$. As well known, Mn^{2+} dissolves into the electrolyte solution while Mn^{4+} remains into the bulk of the electrode. Both

[a]*Department of Chemical Engineering, Iwate University, 4-3-5 Ueda, Morioka, Iwate, 020-8551, Japan*
[b]*Department of WCU Energy Engineering, Hanyang University, Seoul, 133-791, Republic of Korea. E-mail: bruno.scrosati@uniroma1; ityksun@hanyang.ac.kr*
[c]*Department of Chemical Engineering, Hanyang University, Seoul, 133-791, Republic of Korea*
[d]*Dipartimento di Chimica, Università "La Sapienza", 00185 Rome, Italy*

Broader context

Lithium-ion battery researchers envisage that spinel lithium manganese oxide is the most appropriate electrode material to store electricity for large format lithium-ion batteries as power sources for automobiles and solar, wind and wave power plants if the significant problem, capacity fading above ambient temperature, is solved. We think that this issue is circumvented by the particular core-shell morphology developed in this work. Core-shell structures have previously been reported by our and other laboratories. However the strategy developed in this work differs from that used in the past. By using a new synthetic procedure we were able to obtain for the first time a material that did not experience structural mismatch between the core and the shell parts. The particular advanced morphology conferred to the material shows not only a very high reversible capacity based on the particle bulk composition, but also excellent cycling and safety characteristics, which are attributed to the stability of the concentration-gradient outer layer.

these events are deleterious for the performance of the electrode and consequently, of the battery that uses it.[3] The dissolved Mn^{2+} ion deposits as metal Mn on the surface of the negative electrode, thus inhibiting its performance.[4,5] The Mn^{4+} ion promotes film formation of Li_2MnO_3 that is electro-inactive since it induces discontinuity in the networks for electron transfer.[6]

Various strategies have been attempted to overcome this issue. A common one has involved the partial substitution of manganese ions with a series of foreign ions, such as Li, B, Mg, Al, Ni, Co, Fe, Ti, or Zn.[7–15] The goal was to reduce the amount of Mn^{3+} with the final aim of preventing Mn^{2+} dissolution. However, the doping by these ions may result in capacity decrease and in environmental concern. Another popular approach consists in the surface modification of the lithium manganese spinel by an oxide coating, including ZnO, Al_2O_3, Co_3O_4, NiO and BiOF.[16–20] The idea is to provide a shield protecting against manganese dissolution combined with a scavenging action for the fluoride anions eventually present in the electrolyte solution. However, this beneficial effect may be contrasted with an increase of the battery impedance resulting from the insulating nature of the coating media. In the end, none of these strategies have been totally successful in making the lithium manganese spinel electrode viable for practical batteries and in fact, its use is limited to few niche markets.

In this work we report a new strategy and demonstrate its effectiveness in improving the behaviour of lithium manganese spinel electrodes, such as to provide them by an exceptional capacity stability upon cycling in temperature ranges where all the previous manganese-based electrode materials inevitably failed.

2. Experimental

The $MnCO_3$ and $MnCO_3$-$(Ni_{0.25}Mn_{0.75})CO_3$ core-shell compounds were synthesized by a co-precipitation method originally developed in our laboratory.[28] To prepare the core $MnCO_3$, a 2.0 mol L^{-1} aqueous solution of $MnSO_4$ at a concentration of 2.0 mol L^{-1} was pumped into a continuously stirred tank reactor (CSTR, capacity 4 L) under a CO_2 atmosphere. At the same time, a 2.0 mol L^{-1} Na_2CO_3 solution (aq.) and the desired amount of NH_4OH solution (aq. conc. 0.4 mol L^{-1}) chelating agent were also separately fed into the reactor. The concentration of the solution, its pH (7.5), the temperature of operation (50 °C) and the stirring speed of the mixture in the reactor were carefully controlled. Then, an aqueous solution of $NiSO_4$ and $MnSO_4$ (cationic ratio of Ni : Mn = 1 : 3) at a 2.0 mol L^{-1} concentration was continuously pumped into the reactor to completely encapsulate the $MnCO_3$ core. To control the shell thickness, the product was sampled at 1 h intervals up to 3 h. The spherical core-shell $MnCO_3$–$(Ni_{0.25}Mn_{0.75})CO_3$ precursor powder was then filtered and washed. The resulting material was dried at 110 °C. The thus prepared carbonates were fired at 500 °C for 100 h in air to convert the carbonates into oxides. The resulting powders were thoroughly mixed with appropriate amount of lithium carbonate and the mixture was calcined at 720 °C for 15 h in air.

The crystalline phases of the synthesized powders were analyzed with powder X-ray diffraction (XRD, Rigaku, RINT-2000) using Cu-Kα radiation. The XRD data were obtained at $2\theta = 10°$ to 80°, with a step size of 0.03°. The morphology of the prepared powders was determined by scanning electron microscopy (SEM, JSM-6340F, JEOL). The chemical compositions of the final powders were determined by atomic absorption spectroscopy (AAS, Vario 6, AnalyticJena).

Electrochemical testing was performed in R2032 coin-type cells. The positive electrodes were fabricated by blending the prepared powders, Super P® carbon black, and polyvinylidene fluoride (Sigma Aldrich, MW: 534,000 g mol^{-1}) (85 : 7.5 : 7.5) in *N*-methyl-2-pyrrolidone. The slurry was then cast onto an aluminium foil and dried at 110 °C for 10 h in a vacuum oven and then disks were punched out of the foil. The negative electrode was a lithium foil (Honjo Chemical Corporation) and the electrolyte (0.3 ml) a 1 M $LiPF_6$ solution in an ethylene carbonate (EC)–diethyl carbonate (DEC) mixture (3 : 7 ratio by volume, Cheil Industries Inc.). The cells were charged and discharged within a voltage range of 3.0–4.3 V or 3.0–5.0 V at a constant current density of 100 mA g^{-1} and elevated temperature (60 °C). A laminated-type full cell wrapped with an Al pouch (capacity, 10 mAh) was fabricated to evaluate the availability of the electrode with carbon electrode. Mesocarbon microbead graphite (Osaka Gas) was used as the negative electrode. The same electrolyte solution as the coin cell test was used for the full cell test. The positive and negative electrodes were separated by a porous polypropylene film. The cell was cycled between 3 and 4.2 V at a very low rate of 0.01–0.5 C (1.5–40 mA g^{-1}) during the initial formation process. The cells were charged and discharged between 3.0 and 4.2 V by applying a constant 1 C current (10 mA corresponds to 80 mA g^{-1}) at 60 °C.

3. Results and discussion

The approach adopted in this work is based on an innovative core-shell electrode morphology, where a lithium-rich manganese spinel, $Li_{1.1}Mn_{1.9}O_4$ is the core and a high voltage lithium nickel manganese spinel $LiNi_{0.5}Mn_{1.5}O_4$ is the shell. The beneficial effect of this morphology is twofold. The average manganese oxidation state in the shell compound is Mn^{4+}, with no presence of Mn^{3+}: accordingly at the shell there are no conditions for the disproportionate process and thus, for Mn^{2+} dissolution. In addition, the $LiNi_{0.5}Mn_{1.5}O_4$ shell compound is not electrochemically active in the 4 V range of operation of the $Li_{1.1}Mn_{1.9}O_4$ core compound. Consequently, any contact with the electrolyte is prevented and the $Li_{1.1}Mn_{1.9}O_4$ may safely operate with no risk of manganese dissolution.

Fig. 1 shows a scheme for the formation sequence and the architecture of our core-shell electrode formulation. Previous results obtained in our laboratory have shown that spherical morphology is the most appropriate for assuring sediment of foreign material.[21–23] Accordingly, the synthesis started from a spherical $MnCO_3$ core, followed by its complete encapsulation by a $(Ni_{0.25}Mn_{0.75})CO_3$ shell, to the final formation, by thermal lithiation of the core carbonate, of the microscale, spherical $Li_{1.1}Mn_{1.9}O_4$ core–$LiNi_{0.5}Mn_{1.5}O_4$ shell morphology, see experimental section for more details.

The SEM images of Fig. 2a and 2b illustrate the morphology of the precursor and of the final material, respectively. The images show that the shell has an uninterrupted thickness of the order of 2 μm that completely and uniformly covers the core, this

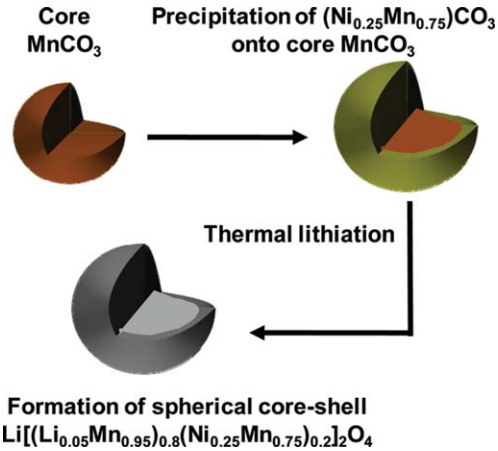

Fig. 1 Scheme of the formation sequence of the core-shell spinel structure.

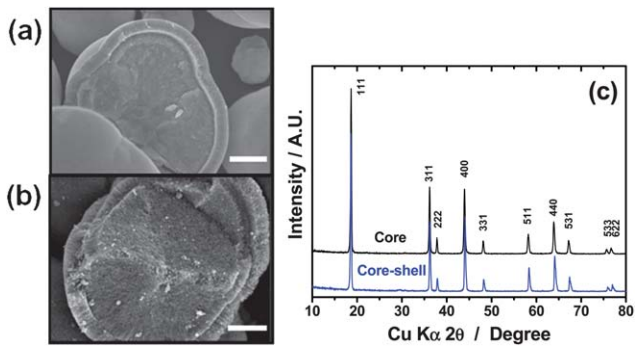

Fig. 2 SEM images of fractured (a) core-shell precursor (scale bar: 5 μm) and (b) lithiated spinel powder (scale bar: 5 μm); (c) XRD patterns of the core $Li_{1.1}Mn_{1.9}O_4$ and the core-shell $Li[(Li_{0.05}Mn_{0.95})_{0.8}(Ni_{0.25}Mn_{0.75})_{0.2}]_2O_4$ powders.

being the unique and main feature of our material. A somewhat similar structure was recently claimed by Li *et al.*[24] However, in their case the coating layer was very thin, *i.e.* of the order of 10–20 nm, and no evidence of a real and effective core-shell configuration was provided.

The structure of our material was controlled by XRD. The pattern confirmed that the material adopts the typical single phase spinel structure in Fig. 2c, although the calculated lattice parameter, 8.205(2) Å, was slightly smaller than that expected for the core $Li_{1.1}Mn_{1.9}O_4$ material, *i.e.* 8.216(1) Å. This minor difference may be ascribed to the presence of $LiNi_{0.5}Mn_{1.5}O_4$ whose lattice parameter, *i.e.*, ~8.17 Å, is smaller than that of $Li_{1.1}Mn_{1.9}O_4$.[25–27] The chemical composition was determined by atomic absorption spectroscopy to be $Li_{1.08}Mn_{1.82}Ni_{0.1}O_4$, which can be represented in the core-shell notation as $Li[(Li_{0.05}Mn_{0.95})_{0.8}(Ni_{0.25}Mn_{0.75})_{0.2}]_2O_4$, namely, $Li_{1.1}Mn_{1.9}O_4$ core–$LiNi_{0.5}Mn_{1.5}O_4$ shell.

Fig. 3 compares the voltage profiles of the discharge (lithium removal)–charge (lithium uptake) cycles at 60 °C, one using the pristine $Li_{1.1}Mn_{1.9}O_4$ electrode (Fig. 3a) and the other $Li[(Li_{0.05}Mn_{0.95})_{0.8}(Ni_{0.25}Mn_{0.75})_{0.2}]_2O_4$ core-shell electrode (Fig. 3b). Both profiles evolve with the two-plateau signature in the 4 V region that is typical for the lithium manganese spinel electrochemical process. The pristine $LiNi_{0.5}Mn_{1.5}O_4$ also exhibits the typical flat two potential plateaus in the 5 V region (Fig. 3a).

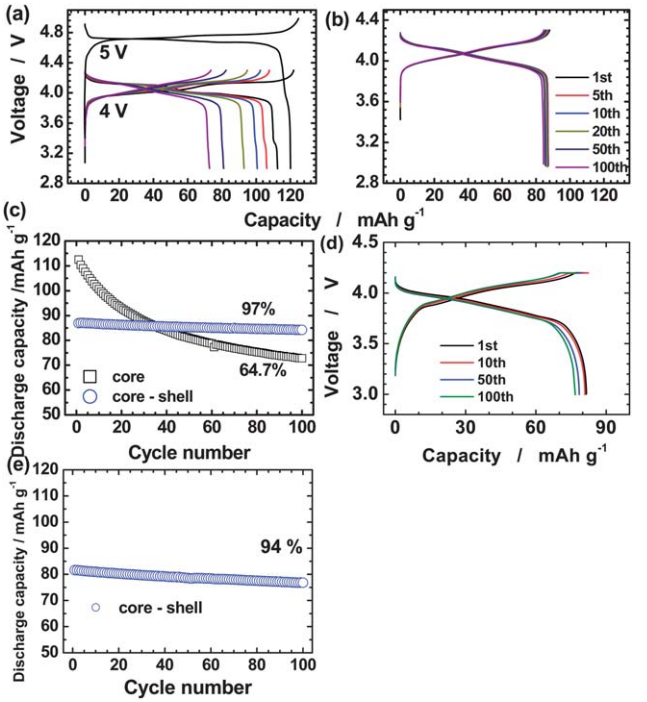

Fig. 3 Continuous charge and discharge curves of (a) the core $Li_{1.1}Mn_{1.9}O_4$ and the first charge and discharge curves of the shell $LiNi_{0.5}Mn_{1.5}O_4$, (b) core-shell $Li/Li[(Li_{0.05}Mn_{0.95})_{0.8}(Ni_{0.25}Mn_{0.75})_{0.2}]_2O_4$ cells at 60 °C performed in an R2032 coin cell, (c) the corresponding cycling performances of the Li/core and core-shell cells at 60 °C, (d) continuous charge and discharge curves of $C/Li[(Li_{0.05}Mn_{0.95})_{0.8}(Ni_{0.25}Mn_{0.75})_{0.2}]_2O_4$ cells at 60 °C, and (e) corresponding cyclability performed in an Al-laminate cell.

However, there is a dramatic difference in the capacity delivery upon cycling: while the cell using the plain $Li_{1.1}Mn_{1.9}O_4$ electrode shows a continuous capacity decay, the one using the core-shell configuration electrode has a very stable capacity delivery with a capacity retention of 97% over 100 cycles, see Fig. 3c.

Fig. 3c also shows that the initial specific capacity of the pristine $Li_{1.1}Mn_{1.9}O_4$ electrode is higher than that of the core-shell electrode. This is not surprising but rather expected since the shell component is not electrochemically active in the voltage range of cell operation, *i.e.* around 4 V. Besides, it is well known from vast literature evidence that coating helps to increase the stability of lithium manganese spinel electrodes, however with a penalty in the capacity value. In case of the $C/Li[(Li_{0.05}Mn_{0.95})_{0.8}(Ni_{0.25}Mn_{0.75})_{0.2}]_2O_4$ full cell, the operation voltage on discharge is maintained during cycling (Fig. 3d). Moreover, the capacity retention of the core-shell particles during the extensive cycling is approximately 94% of its initial capacity (Fig. 3e), although the $C/Li_{1.1}Mn_{1.9}O_4$ cell gave disappointing cycling performance in the temperature.[17] In this respect it is to be noted that, to the best of our knowledge, the specific capacity of our core-shell electrode material is higher than any other previously obtained with alternative oxide-coated electrodes.[16–20]

The results reported in Fig. 3 clearly confirm the expected protecting action of the shell layer over the core material. This was finally demonstrated by XRD analyses taken at the end of the electrodes' cycle life shown in Fig. 4 and Table 1. The pattern of the pristine $Li_{1.1}Mn_{1.9}O_4$ reveals the coexistence of the original

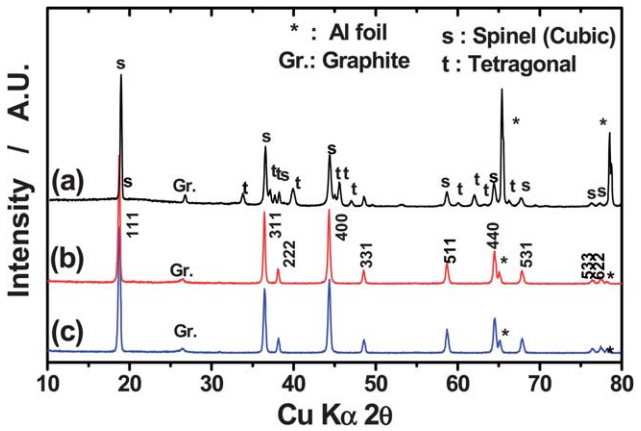

Fig. 4 Powder XRD patterns of extensively cycled (a) core $Li_{1.1}Mn_{1.9}O_4$ (3–4.3 V), and microscale spherical core-shell $Li[(Li_{0.05}Mn_{0.95})_{0.8}$-$(Ni_{0.25}Mn_{0.75})_{0.2}]_2O_4$ in voltage range of (b) 3–4.3 V and (c) 3–5 V.

cubic phase with the tetragonal phase, this being a clear indication of that the Mn^{2+} disproportionation/dissolution had occurred, probably by HF attack from the electrolyte. On the contrary, the XRD pattern of the core-shell material shows that the original cubic structure was maintained throughout the cycling test to 4.3 V and even to 5 V at 60 °C, with no evidence of tetragonal phase. The lattice parameter after cycling was a = 8.201(5) Å, *i.e.*, a value very close to that of the fresh material, a = (8.205(2) Å).

Attack of HF to the surface of the core-shell particles may not be excluded; however, the eventual damaged parts do not affect the delivery capacity since the shell is electrochemically inactive in the 4 V operating range. Furthermore, the thick shell is likely to protect the core material from HF attack during the cycling. All the above discussed experimental evidences concur to demonstrate that ours is a winning strategy for protecting the lithium manganese spinel electrode, conferring to it a very high stability and a superior cycling performance even at high temperatures. An additional feature of the core-shell electrode morphology here proposed is that, in addition to the $Li_{1.1}Mn_{1.9}O_4$ core component, the $LiNi_{0.5}Mn_{1.5}O_4$ shell component can also be electrochemically active and thus, contribute to the overall capacity. Fig. 5a shows the charge–discharge voltage profiles of a lithium cell galvanostatically cycled at 60 °C over a 3.0–5.0 V, namely in a voltage range where both components are electrochemically active. The two representative mixed

Table 1 Calculated lattice parameters based on Fig. 4

		Lattice parameter/Å	
	Space group	*a*-axis/Å	*c*-axis/Å
Core $Li_{1.1}Mn_{1.9}O_4$ core-shell	$Fd\bar{3}m$	8.147(6)	—
	$I4_1/amd$	5.664(4)	9.086(7)
$Li[(Li_{0.05}Mn_{0.95})_{0.8}$-$(Ni_{0.25}Mn_{0.75})_{0.2}]_2O_4$ (cycled 3–4.3 V) core-shell	$Fd\bar{3}m$	8.201(5)	—
$Li[(Li_{0.05}Mn_{0.95})_{0.8}$-$(Ni_{0.25}Mn_{0.75})_{0.2}]_2O_4$ (cycled 3–5 V)	$Fd\bar{3}m$	8.184(6)	—

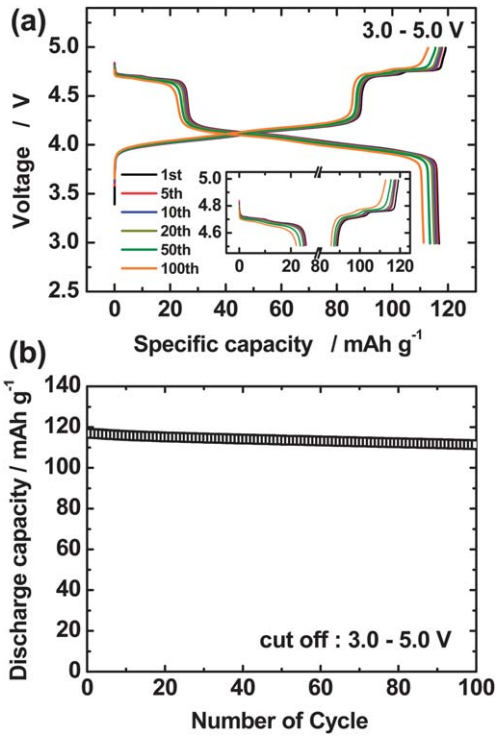

Fig. 5 (a) Continuous charge and discharge curves of the core-shell and (b) cycling performance at 60 °C over a voltage range of 3.0–5.0 V.

charge-discharge curves are clearly shown: one evolving with a 5V plateau associated with the shell component and a following one evolving with a 4V plateau associated with the core component. The total capacity amounts to 116.8 mAh g^{-1} of which 26 mAh g^{-1} is provided by the upper 5V plateau.

Fig. 5b concurs to definitely demonstrate the unique feature of the $Li[(Li_{0.05}Mn_{0.95})_{0.8}(Ni_{0.25}Mn_{0.75})_{0.2}]_2O_4$ core-shell electrode developed in this work. The electrode has an exceptional capacity retention upon cycling at 60 °C, namely of the order of 95.2% over 100 cycles. In addition, the initial irreversible capacity, a deleterious phenomenon that affects most of the cathode materials, is here confined to only 2.1%. To our knowledge, such a high performance is rarely found in common lithium ion battery chemistry and this is further evidence of the practical relevance of our core-shell structure. The stability of this electrode structure is further confirmed by Fig. 6 that shows the SEM image of a cross-section of a particle of the $Li[(Li_{0.05}$-$Mn_{0.95})_{0.8}(Ni_{0.25}Mn_{0.75})_{0.2}]_2O_4$ core-shell electrode taken after the 100 cycles test of Fig. 5. The image demonstrates that the initial morphology is kept throughout the cycling test with no evidence of structural mismatch nor of separation or breakage between the core and shell.

Finally, it is important to point out the last but not least bonus of the core-shell structure here reported. Despite the fact that in the course of the extended cycling test the spinel core is periodically exposed to high overcharge conditions, no fluctuations or voltage profile nor abrupt capacity fading is observed, see Fig. 5a and 5b. This strongly suggests that the outer $LiNi_{0.5}Mn_{1.5}O_4$ shell, in addition to the series of beneficial actions above discussed, also confers overcharge protection by shuttling

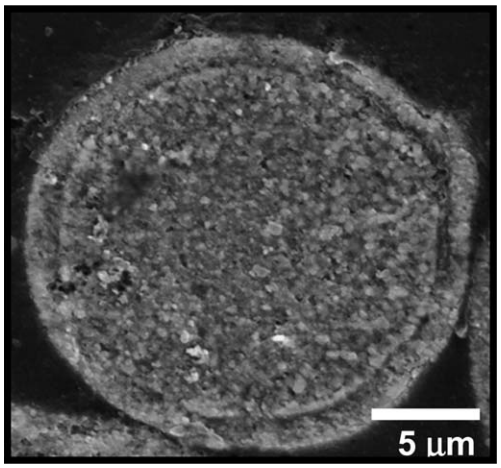

Fig. 6 SEM image of extensively cycled (3–5 V) microscale spherical core-shell $Li[(Li_{0.05}Mn_{0.95})_{0.8}(Ni_{0.25}Mn_{0.75})_{0.2}]_2O_4$ particle.

lithium ions in and out when the charge cut-off limit of $Li[(Li_{0.05}Mn_{0.95})_{0.8}(Ni_{0.25}Mn_{0.75})_{0.2}]_2O_4$ core-shell electrode hits 4.7 V.

5. Conclusions

In conclusion, we demonstrate in this work that, by exploiting an original co-precipitation synthetic procedure, new core-shell $Li[(Li_{0.05}Mn_{0.95})_{0.8}(Ni_{0.25}Mn_{0.75})_{0.2}]_2O_4$ electrode configurations, with unique properties in terms of cycling stability at high temperatures, can be obtained. We believe that these properties are superior to those provided by any lithium manganese spinel-based electrode so far reported. This breakthrough is expected to definitely contribute to making lithium manganese spinel electrodes viable for practical applications in advanced lithium ion batteries.

Acknowledgements

This research was supported by WCU (World Class University) program through the Korea Science and Engineering Foundation by Education, Science, and Technology (R31-2008-000-10092) and the National Research Foundation of Korea (NRF) grant funded by the Korea government (MEST) (No. 2009-0092780).

References

1 J. M. Tarascon and M. Armand, *Nature*, 2001, **414**, 359–367.
2 J. Arai, T. Yamaki, S. Yamauchi, T. Yuasa, T. Maeshima, T. Sakai, M. Koseki and T. Horiba, *J. Power Sources*, 2005, **146**, 788–792.
3 R. J. Gummow, A. de Kock and M. M. Thackeray, *Solid State Ionics*, 1994, **69**, 59–67.
4 A. Blyr, C. Sigala, G. Amatucci, D. Guyomard, Y. Chabre and J. M. Tarascon, *J. Electrochem. Soc.*, 1998, **145**, 194–209.
5 S. Komaba, N. Kumagai and Y. Kataoka, *Electrochim. Acta*, 2002, **47**, 1229–1239.
6 Y.-K. Sun, G.-S. Park, Y.-S. Lee, M. Yoshio and K. S. Nahm, *J. Electrochem. Soc.*, 2001, **148**, 994–998.
7 J. M. Tarascon, E. Wang, F. K. Shokoohi, W. R. McKinnon and S. Colson, *J. Electrochem. Soc.*, 1991, **138**, 2859–2864.
8 J. M. Tarascon, W. R. McKinnon, F. Coowar, T. N. Bowmer, G. Amatucci and D. Guyomard, *J. Electrochem. Soc.*, 1994, **141**, 1421–1431.
9 A. D. Robertson, S. H. Lu, W. F. Averill and W. F. Howard Jr, *J. Electrochem. Soc.*, 1997, **144**, 3500–3505.
10 J. H. Lee, J. K. Hong, D. H. Jang, Y.-K. Sun and S. M. Oh, *J. Power Sources*, 2000, **89**, 7–14.
11 S.-T. Myung, S. Komaba and N. Kumagai, *J. Electrochem. Soc.*, 2001, **148**, A482–A489.
12 K. Amine, H. Tukamoto, H. Yasuda and Y. Fujita, *J. Electrochem. Soc.*, 1996, **143**, 1607–1613.
13 K. Amine, H. Tukamoto, H. Yasuda and Y. Fujita, *J. Power Sources*, 1997, **68**, 604–608.
14 M. Hosoya, H. Ikuta, T. Uchida and M. Wakihara, *J. Electrochem. Soc.*, 1997, **144**, L52–L53.
15 G. Amatucci, A. Du Pasquier, A. Blyr, T. Zheng and J. M. Tarascon, *Electrochim. Acta*, 1999, **45**, 255–271.
16 Y.-K. Sun, K.-J. Hong and J. Prakash, *J. Electrochem. Soc.*, 2003, **150**, A970–A972.
17 S.-T. Myung, K. Hosoya, S. Komaba, H. Yashiro, Y.-K. Sun and N. Kumagai, *Electrochim. Acta*, 2006, **51**, 5912–5919.
18 S.-T. Myung, K. Izumi, S. Komaba, Y.-K. Sun, H. Yashiro and N. Kumagai, *Chem. Mater.*, 2005, **17**, 3695–3704.
19 K.-S. Lee, S.-T. Myung, H. J. Bang and Y.-K. Sun, *J. Power Sources*, 2009, **189**, 494–498.
20 K.-S. Lee, S.-T. Myung, K. Amine, H. Yashiro and Y.-K. Sun, *J. Mater. Chem.*, 2009, **19**, 1995–2005.
21 Y.-K. Sun, S.-T. Myung, B.-C. Park, J. Prakash, I. Belharouak and K. Amine, *Nat. Mater.*, 2009, **8**, 320–324.
22 Y.-K. Sun, S.-T. Myung, M.-H. Kim, J. Prakash and K. Amine, *J. Am. Chem. Soc.*, 2005, **127**, 13411–13418.
23 Y.-K. Sun, S.-T. Myung, B.-C. Park and K. Amine, *Chem. Mater.*, 2006, **18**, 5159–5163.
24 X. Li, Y. Xu and C. Wang, *Appl. Surf. Sci.*, 2009, **255**, 5651–5655.
25 S.-T. Myung, S. Komaba, N. Kumagai, H. Yashiro, H.-T. Chung and T.-H. Cho, *Electrochim. Acta*, 2002, **47**, 2543–2549.
26 J.-H. Kim, S.-T. Myung, C. S. Yoon, S. G. Kang and Y.-K. Sun, *Chem. Mater.*, 2004, **16**, 906–914.
27 H. J. Bang, V. S. Donepudi and J. Prakash, *Electrochim. Acta*, 2002, **48**, 443–451.
28 S.-H. Park, H.-S. Shin, S.-T. Myung, C. S. Yoon, K. Amine and Y.-K. Sun, *Chem. Mater.*, 2005, **17**, 6–8.